Published in final edited form as:

Nat Med. 2016 May ; 22(5): 524–530. doi:10.1038/nm.4075.

Nod2-mediated recognition of the microbiota is critical for mucosal adjuvant activity of cholera toxin

Donghyun Kim[1], **Yun-Gi Kim**[1], **Sang-Uk Seo**[1], **Dong-Jae Kim**[1], **Nobuhiko Kamada**[2], **Dave Prescott**[3], **Dana J. Philpott**[3], **Philip Rosenstiel**[4], **Naohiro Inohara**[1], and **Gabriel Núñez**[1]

[1]Department of Pathology and Comprehensive Cancer Center, University of Michigan Medical School, Ann Arbor, Michigan, USA

[2]Division of Gastroenterology, Department of Internal Medicine, University of Michigan Medical School, Ann Arbor, Michigan, USA

[3]Department of Immunology, University of Toronto, Toronto, Canada

[4]Institute of Clinical Molecular Biology; University of Kiel, Kiel, Germany

Abstract

Cholera toxin (CT) is a potent adjuvant for inducing mucosal immune responses. However, the mechanism by which CT induces adjuvant activity remains unclear. Here we show that the microbiota is critical for inducing antigen-specific IgG production after intranasal immunization. After mucosal vaccination with CT, both antibiotic-treated mice and germ-free (GF) had reduced antigen-specific IgG, recall-stimulated cytokine responses, an impaired follicular helper T (T_{FH}) response and reduced plasma cells. Recognition of symbiotic bacteria via Nod2 in $CD11c^{+}$ cells was required for the adjuvanticity of CT. Reconstitution of GF mice with a Nod2 agonist or *Staphylococcus sciuri* having high Nod2-stimulatory activity was sufficient to promote robust CT adjuvant activity whereas bacteria with low Nod2-stimulatory activity did not. Mechanistically, CT enhanced Nod2-mediated cytokine production in DCs via intracellular cAMP. These results show an important role for the microbiota and the intracellular receptor Nod2 in promoting the mucosal adjuvant activity of CT.

Cholera toxin (CT), an enterotoxin secreted by *Vibrio cholera* that is responsible for the diarrhea associated with cholera, is a potent mucosal adjuvant for stimulating antigen-specific responses when given by nasal or oral routes[1–3]. CT is composed of pentameric B subunits that bind to the cell surface GM1 ganglioside receptor, and a monomeric A catalytic

Corresponding authors: Yun-Gi Kim (; Email: yungikim77@gmail.com) and Gabriel Nuñez (; Email: gabriel.nunez@umich.edu)

Author Contributions

D.K., Y.-G.K., and G.N. conceived the study. D.K. performed most of the experiments. Y-G.K. performed several experiments. S.-U.S. and D.-J.K. helped with experiments. D.P., D.J.P., and P.R. generated and performed initial characterization of *Cd11c*^{Cre};*Nod2*$^{fl/fl}$ mice. N.K., D.J.P., P.R., and N.I. helped in the design of several experiments and provided critical advice. D.K. and G.N. wrote the manuscript with contributions from all authors.

Competing financial interests

The authors declare no competing financial interests.

subunit that activates the heterotrimeric guanine nucleotide binding protein Gsα which in turn stimulates cAMP production by adenylate cyclase[1,4,5]. Several studies have linked the adjuvant effect of CT to the catalytic activity of the monomeric A subunit and the ADP-ribosylation of Gs[4,5]. Although toxicity of CT prevents its implementation in the clinic, understanding the mechanisms underlying its potent adjuvant activity may lead to the development of nontoxic and effective adjuvants for mucosal vaccination.

A number of studies have revealed that mononuclear phagocytes including dendritic cells (DCs) are critical targets for the adjuvant activity of CT[3,6,7]. CT is considered a potent T helper type 2 (T_H2) adjuvant because it stimulates T_H2-associated cytokines and robust IgG_1 production[8–10]. CT can inhibit interleukin-12 (IL-12) production and differentiation of plasmacytoid DCs and $CD8\alpha^+$ conventional DCs through the induction of intracellular ATP in DCs[8,11]. However, other studies have shown that intracellular cAMP and Gsα positively regulate T_H1 and T_H17 immune responses[7,12]. Furthermore, CT can act via Gsα within $CD11b^+$ DCs to promote $T_H1/T_H2/T_H17$ responses, but IL-12 and IL-17 are dispensable for the adjuvant activity of CT[13]. Collectively, these studies indicate that CT acts on monuclear phagocytes to mediate its adjuvant activity, but the precise cellular and molecular mechanisms by which CT promotes antigen-specific antibody responses remain poorly understood.

Members of the nucleotide-binding oligomerization domain-like receptor (NLR) family function as intracellular pattern recognition receptors (PRRs) to activate immune responses in response to microbial and damage-associated stimuli[14]. The NLR family member Nod2 recognizes peptidoglycan molecules containing muramyl dipeptide (MDP) that are produced by both Gram-negative and Gram-positive bacteria[15,16]. Upon MDP recognition, Nod2 induces the activation of the nuclear factor κB (NF-κB) and the mitogen-activated protein kinases (MAPKs) via the receptor-interacting serine/threonine-protein kinase 2 (Ripk2) to induce pro-inflammatory and anti-microbial molecules[17,18]. Upon systemic stimulation, MDP-induced Nod2 activation induces predominantly T_H2-cell-dependent humoral immune responses and in combination with toll-like receptor (TLR) agonists promotes T_H1 and T_H2 immune responses in mice[19–21]. However, the role of Nod2 in promoting mucosal adjuvant activity remains poorly understood. Here, we show that the microbiota plays a role in the mucosal adjuvant activity of CT. The effect of the microbiota was mediated through the recognition of symbiotic bacteria by Nod2 in CD11c-expressing phagocytes.

Results

Symbiotic bacteria promote the adjuvant activity of cholera toxin

The nasal cavity of mammals harbors a rich community of symbiotic bacteria[22]. To assess the role of such bacteria in the adjuvant activity of CT, mice were intranasally treated with a cocktail of antibiotics (ampicillin, neomycin, metronidazole, and vancomycin) once one week before immunization followed by administration of the same antibiotic cocktail in the drinking water ad libitum for three weeks. The treatment resulted in a depletion of bacteria, including a greater than 500-fold decrease of cultivatable bacteria in the nasal lavage fluid (NALF) 2 weeks post immunization (data not shown). Antibiotic-treated and untreated mice were intranasally immunized with the model antigen, human serum albumin (HSA), and CT

and 2 weeks later sera were collected and analyzed for HSA-specific IgG by ELISA. As expected, no antigen-specific IgG was detected in the plasma of mice immunized with HSA in the absence of CT (Supplementary Fig. 1) while immunization with HSA and CT induced robust antigen-specific IgG (Fig. 1a). Depletion of bacteria with antibiotics suppressed the production of HSA-specific IgG as compared to untreated mice (Fig. 1a). After *ex vivo* restimulation of splenocytes with antigen, production of the T_H1 cytokine IFN-γ and the T_H2 cytokine IL-5 were increased in splenocytes from mice untreated with antibiotics, but not in splenocytes from antibiotic-treated mice (Fig. 1b).

To examine the contribution of the microbiota in mucosal immunization via a different route, we performed oral immunization with HSA and CT in antibiotic-treated and untreated mice. Similar to the results with nasal immunization, bacterial depletion impaired the induction of HSA-specific IgG in plasma as well as the production of IL-5 and IFN-γ by restimulated splenocytes when mice were orally immunized with HSA and CT (Supplementary Fig. 2). In contrast, intraperitoneal immunization with HSA induced comparable antigen-specific IgG responses in antibiotic-treated and untreated mice (Supplementary Fig. 3). In addition, we assessed the role of symbiotic bacteria after intranasal immunization with HSA together with CpG (a TLR9 agonist) or MALP-2 (a TLR2 agonist) instead of CT in antibiotic-treated and untreated mice. Treatment with antibiotics reduced HSA-specific IgG production when CpG was used as adjuvant, but had no or minimal effect in mice treated with MALP-2 (Supplementary Fig. 4). These results suggest that the route of immunization is important for the ability of the microbiota to enhance the adjuvant activity of CT. Furthermore, the microbiota can enhance the adjuvant activity of some, but not all, adjuvants in the nasal cavity. To confirm a role for symbiotic bacteria in the mucosal adjuvanticity of CT, specific pathogen-free (SPF) and germ-free (GF) mice were intranasally immunized with HSA and CT. Primary and secondary HSA-specific IgG responses were impaired in GF mice as compared to SPF mice harboring a microbiota (Fig. 1c, d). Furthermore, the production of IFN-γ and IL-5 induced upon re-stimulation of splenocytes with antigen was abrogated in splenocytes from GF mice (Fig. 1e). These results indicate that symbiotic bacteria play a role in promoting the adjuvant activity of CT after intranasal immunization.

Nod2-Ripk2 mediates the adjuvant activity of cholera toxin

Bacteria are sensed by host PRRs including TLRs and NLRs which leads to the induction immune responses[14,23,24]. To assess which PRR is involved in the recognition of bacteria during intranasal immunization with CT, we intranasally immunized wild-type (WT) mice and mutant mice deficient in Myd88, an adaptor for signaling via TLR and IL-1/18 receptors, and mice lacking Ripk2, the adaptor required for Nod1/Nod2 signaling[14,23]. Deficiency in Ripk2, but not Myd88, impaired HSA-specific IgG responses induced by intranasal immunization with CT (Fig. 2a, b). Because Ripk2 mediates both Nod1 and Nod2 signaling, we next tested the ability of CT to promote antigen-specific IgG in *Nod1*$^{-/-}$ and *Nod2*$^{-/-}$ mice. Antigen-specific IgG responses induced by nasal immunization with HSA and CT were impaired in *Nod2*$^{-/-}$ mice, but not in *Nod1*$^{-/-}$ animals (Fig. 2c–e). HSA-specific IgG_1, IgG_{2b} and IgM were also reduced in *Nod2*$^{-/-}$ mice after intranasal immunization with HSA and CT (Supplementary Fig. 5). Furthermore, the production of IFN-γ and IL-5 induced by restimulation of splenocytes with antigen was impaired in

Nod2$^{-/-}$ mice (Fig. 2f). When mice were intranasally immunized with higher amounts of HSA and CT, HSA-specific IgG responses were still reduced in *Nod2*$^{-/-}$ mice when compared to WT mice (Supplementary Fig. 6a). Moreover, HSA-specific IgA production in the nasal cavity was also reduced in *Nod2*$^{-/-}$ mice (Supplementary Fig. 6b). In contrast, *Ripk2*$^{-/-}$ and *Nod2*$^{-/-}$ mice mounted normal antigen-specific IgG responses when immunized intraperitoneally with HSA together with CT or alum, respectively (Supplementary Fig. 7).

DCs play a role in promoting the adjuvant activity of CT[13]. Analyses of cells in the nasal-associated lymphoid tissue (NALT) showed that the CD45^{+}CD11c^{+} cell population expressed higher amounts of *Nod2* mRNA than the CD45^{+}CD11c^{-} or CD45^{-}CD11c^{-} cell populations (Supplementary Fig. 8), suggesting that CD11c^{+} DCs or macrophages could play a role in response to Nod2 agonist. To determine whether Nod2 acts within phagocytes including DCs, we immunized control mice and *Cd11c*^{Cre};*Nod2*$^{fl/fl}$ mice in which Nod2 was deleted in CD11c^{+} cells (Supplementary Fig. 9). HSA-specific IgG responses were impaired in *Cd11c*^{Cre};*Nod2*$^{fl/fl}$ mice after intranasal immunization with CT (Fig. 2g). In contrast, HSA-specific IgG production in response to immunization with CT was not altered in *K14*^{Cre};*Nod2*$^{fl/fl}$ mice with Nod2 deletion in keratinized epithelia (Supplementary Fig. 10). These results indicate that Nod2 acts within CD11c^{+} phagocytes to promote the adjuvant activity of CT.

Nod2 is required for the generation of T_{FH} cells and plasma cells

Follicular helper T (T_{FH}) cells mediate the generation and maintenance of germinal centers as well as the survival and selection of B cells that differentiate into plasma cells capable of producing high affinity antibodies against foreign antigen[25–27]. As Nod2 was important for antigen-specific IgG production, we examined whether Nod2 regulates the generation of T_{FH} cells and plasma cells after intranasal immunization with CT. The percentage and total number of T_{FH} cells (CXCR5^{+}PD-1^{hi}) and plasma cells (CD19^{+}CD138^{+}IgD^{-}) were reduced in the draining lymph nodes of *Nod2*$^{-/-}$ mice immunized intranasally with CT and HSA when compared to WT mice (Fig. 3a–f). Furthermore, ELISPOT assay revealed that Nod2 deficiency decreased the number of cells producing HSA-specific IgG in the draining lymph nodes of immunized mice (Fig. 3g). These results indicate that Nod2 regulates the generation of T_{FH} cells and plasma cells after intranasal immunization with CT.

Cholera toxin enhances Nod2-induced cytokine production in DCs

Pretreatment of DCs with CT inhibits the ability of DCs to produce cytokines in response to TLR agonists including lipopolysaccharide[8,11]. To determine whether CT regulates Nod2-induced cytokine production, we treated DCs with CT in the presence or absence of MDP, a Nod2 agonist. Treatment with CT enhanced MDP-induced IL-6, IL-23, and IL-12p40 production in DCs (Fig. 4a). The ability of CT to enhance MDP-induced cytokine production required Nod2 (Fig. 4a) and Ripk2, the adaptor kinase required for Nod2 signaling (Fig. 4b). Thus, CT enhances Nod2-induced cytokine production in DCs.

Cholera toxin enhances Nod2 activation via cAMP/PKA

CT activates adenylate cyclase resulting in increased concentrations of intracellular cAMP[1,5]. To determine whether cAMP regulates Nod2-induced cytokine production, we treated DCs with 8-Br-cAMP, a cell-permeable cAMP analog, in the absence or presence of MDP. As observed with CT, 8-Br-cAMP enhanced the secretion of IL-6, IL-23, and IL-12p40 cytokines in the presence of MDP (Fig. 5a). Moreover, both CT and cAMP enhanced the expression of Nod2 mRNA in DCs (Supplementary Fig. 11).

The effects of increased intracellular cAMP are mediated by protein kinase A (PKA) and exchange protein directly activated by cAMP (EPAC)[7,12]. To clarify the pathway involved in the regulation of MDP-induced responses by CT, DCs were treated with specific activators of each pathway together with MDP. Co-treatment with N6-benzoyl-cAMP, an activator of PKA, and MDP enhanced cytokine production, whereas 8-CPT-2'-O-Me-cAMP, an activator of Epac, did not (Fig. 5b). These results suggest that CT enhances Nod2-induced cytokine production via a cAMP/PKA-dependent mechanism in DCs[28].

NOD2-stimulatory bacteria boost the adjuvanticity of cholera toxin

To test whether MDP can mediate the adjuvant activity of CT in the absence of a microbiota, we immunized GF mice intranasally with HSA in the presence of MDP, CT, or MDP plus CT and anti-HSA IgG responses were measured after intranasal stimulation. The combination of MDP and CT induced robust antigen-specific IgG, but MDP or CT alone did not (Fig. 6a). There was a marginal increase in HSA-specific IgG in GF mice stimulated with CT when compared with MDP alone (Fig. 6a), suggesting that CT can induce low amounts of antigen-specific IgG in the absence of the microbiota.

We next assessed the presence of Nod2-stimulatory activity in the NALF using a reporter assay[29]. Nod2-stimulatory activity was detected in the NALF from SPF mice (Fig. 6b). These experiments suggested that the nasal cavity is inhabited by bacteria which produce peptidoglycan molecules containing MDP. To identify bacteria producing Nod2-stimulatory activity, we isolated bacterial colonies from the NALF of mice and analyzed individual bacteria for Nod2-stimulatory activity and their taxa by 16S RNA gene sequencing. Some bacterial species isolated from the nasal cavity including *Staphylococcus sciuri* and *Bacillus clausii* exhibited robust Nod2-stimulatory activity whereas *Bordetella hinzii, Staphylococcus gallinarum* and *Bacillus pumilus* stimulated less Nod2 activity (Fig. 6c). To compare the contribution of bacteria possessing high and low Nod2-stimulatory activity to the adjuvanticity of CT, we intranasally inoculated SPF mice with live *S. sciuri* or *S. gallinarum* together with HSA and CT. Colonization of the nasal cavity of mice with *S. sciuri*, that exhibited robust Nod2-stimulatory activity, enhanced antigen-specific IgG response after immunization with HSA and CT whereas colonization with *S. gallinaum* induced little or no significant adjuvant activity (Fig. 6d and Supplementary Fig. 12). Furthermore, monocolonization of the nasal cavity of GF mice with *S. sciuri* enhanced the adjuvanticity of CT (Fig. 6e). To test whether bacteria can act locally, we inoculated the nasal cavity of GF mice with small amounts of individual UV-inactivated bacteria in addition to HSA and CT. Inoculation of GF mice with *S. sciuri* or *B. clausii* having high Nod2-stimulatory activity enhanced the adjuvant activity of CT, whereas inoculation with *S. gallinaum* or *E. coli* did

not (Fig. 6f and Supplementary Fig. 13). *S. sciuri* enhanced the adjuvant activity of CT in GF WT mice but not GF *Nod2*$^{-/-}$ mice (Fig. 6g). Taken together, these results indicate that nasal bacteria promote the adjuvant activity of CT through Nod2 in the nasal cavity.

Discussion

There is mounting evidence that the microbiota plays a critical role in the development and function of the host immune system including the development of T_H17 cells, regulatory T (T_{reg}) cells, and IgA-producing B cells[30,31]. Furthermore, the microbiota can influence the immune response to viral and bacterial infections[32,33]. A notable finding of our studies is the role of the microbiota and Nod2 in the regulation of the adjuvant activity of CT. MDP, the Nod2 agonist, was originally identified as the active component of complete Freund's adjuvant and is sufficient for eliciting adjuvant activity[34]. MDP acts predominantly as a T_H2-polarizing adjuvant, but enhances T_H1 and T_H2 immune responses in the presence of TLR agonists[19–21]. Thus, the ability of CT to promote T_H2-skewed humoral immunity could be explained, at least partly, by MDP-induced immune responses via Nod2. Administration of MDP in the nasal cavity of GF mice was sufficient for CT to elicit adjuvant activity. Furthermore, the adjuvant activity of CT was restored in WT but not *Nod2*$^{-/-}$ GF mice colonized with nasal bacteria producing MDP. Collectively, these results indicate that the presence of Nod2-stimulatory bacteria colonizing the nasal cavity is critical for the adjuvant activity of CT. However, it is possible that the adjuvant activity of CT also involves stimulation via TLRs, given that MDP promotes broader immune responses in the presence of TLR agonists[19–21]. In contrast to the immunization via nasal and oral routes, we found no role of the microbiota and Nod2 in the adjuvanticity of CT via intraperitoneal route. Because the intraperitoneal cavity is considered to be free of bacteria, the results suggest that the microbiota may be not essential for the adjuvanticity of CT. However, the microbiota enhances the adjuvant ability of CT via Nod2 stimulation. This function is important in mucosal surfaces where there are abundant symbiotic bacteria producing Nod2 ligands including nasal and gastrointestinal cavities, but not in the peritoneum that is devoid of bacteria. Additionally, it is possible that small amounts of microbial molecules present in the CT preparation may contribute to the adjuvanticity of CT after intraperitoneal immunization, because typically higher doses of CT are used to induce systemic adjuvant activity.

Mononuclear phagocytes including DCs are critical cellular targets of CT to mediate its adjuvant activity *in vivo*[3,6,7]. In line with these findings, we found that Nod2 deficiency in $CD11c^+$ cells impaired the ability of CT to promote antigen-specific IgG after intranasal immunization. Thus, the adjuvanticity of CT may be explained by its ability to stimulate MDP-mediated immune responses in $CD11c^+$ phagocytes like DCs. Consistent with this notion, stimulation of DCs with CT enhanced MDP-induced cytokine responses through a cAMP/PKA-dependent mechanism. CT enhanced MDP-induced IL-6, IL-23, and IL-12p40 production in DCs. However, the MDP-induced immune responses that are critical for the adjuvant activity of CT remain unclear. In models of systemic immunization, Nod2 stimulation by MDP induces OX40 ligand, which is important for T_H2-cell-oriented acquired immunity[35,36]. IL-6 in conjunction with IL-21 promotes optimal T_{FH} responses and development of germinal center B cells[26,27]. IL-12 facilitates the differentiation of T_{FH} cells accompanied by the increase of IL-21, CXCR5 and ICOS, and promotes antibody

production[37,38]. However, IL-12 and IL-17 are dispensable for adjuvant activity CT induced after intranasal immunization[13]. Thus, it is likely that the ability of CT to induce adjuvant activity involves multiple cytokines or activities that remain to be identified. Because both CT and cAMP increased the expression of Nod2 mRNA in DCs, the ability of CT to induce Nod2 expression in DCs may explain, at least partly, the enhancement of MDP-mediated immune responses induced by CT.

One implication of our results is that the microbiota plays a role in immune responses induced by immunization with adjuvants. In developing countries, there is evidence of reduced efficacy of humoral immune responses induced by oral vaccines when compared to industrialized countries[39–41]. Although the reasons for the reduced efficacy of vaccines in developing countries is likely complex, the wide variation in antigen-specific antibody responses cannot be explained solely by nutritional differences[42–44]. Given that the composition of the microbiota in each individual is normally stable throughout life but highly variable among individuals[45], it is possible that the microbiota impacts the effectiveness of vaccines[40,46]. Likewise, changes in the microbiota that occur during lifetime including antibiotic treatment, infection, or subtle changes during aging[22,40,45] may contribute to individual variability and efficacy of vaccination. Consistent with this notion, probiotics can influence immune responses induced by vaccines in animal models[47]. We found that the microbiota can enhance the adjuvant activity of CpG in the nasal cavity, indicating that the ability of the microbiota to regulate adjuvanticity is not limited to CT. Likewise, TLR5 recognition of the microbiota contributes to antibodies responses in response to parenteral influenza vaccination[48]. TLR5-mediated recognition of the microbiota regulated IgG responses in unadjuvanted vaccines, but not those induced by alum or attenuated viral vaccines[48]. In the unadjuvanted influenza subunit vaccines, the microbiota appears to provide adjuvant activity via TLR5 stimulation[48]. In contrast, the adjuvanticity of CT in the nasal cavity is enhanced by the presence of bacteria producing Nod2 agonists and involves increased Nod2 activation in $CD11c^+$ phagocytes. Collectively, these studies suggest that the microbiota can influence humoral immune responses to vaccination via different mechanisms. Although more studies are needed, our studies suggest that environmental and genetic factors that affect the composition of the microbiota may be important factors in determining the capacity of mucosal vaccines to develop protective immunity. Furthermore, understanding of the microbial populations and factors that regulate the immune responses to vaccines may provide insight for the development of more effective vaccination protocols.

Online Methods

Mice

WT C57BL/6, *Myd88*$^{-/-}$, *Ripk2*$^{-/-}$, *Nod1*$^{-/-}$, *Nod2*$^{-/-}$, *Cd11c*^{Cre};*Nod2*$^{fl/fl}$ and *K14*^{Cre};*Nod2*$^{fl/fl}$ mice on the C57BL/6 background were bred and kept under specific pathogen-free (SPF) conditions at the University of Michigan Animal Facility. Conditional *Nod2*$^{fl/fl}$ mice were generated in collaboration with GenOway, France using 129SV ES cells. The proximal loxP site was inserted within intron 1 of the *Nod2* gene, the distal loxP site was introduced together with an FRT flanked neomycin selection cassette within intron 3.

The resultant mouse line was bred with FLP deleter-mice ubiquitously expressing Flp-recombinase to remove the neomycin selection cassette, creating a *Nod2*$^{fl/+}$ mouse in which the region between exon 2 and 3 was flanked by two loxP sites. We backcrossed mice onto the C57BL/6 background for 10 generations. Conditional deletion of the allele using Cre-recombinase results in a deletion of a genomic region of approximately 2 kb carrying both exon 2 (cryptic start codon) and 3 (canonical start codon). GF WT and *Nod2*$^{-/-}$ mice on the C57BL/6 background were bred and maintained at the Germ Free Animal Core Facility of the University of Michigan. Mice were allocated randomly into experimental groups. No blinding was done for animal experiments. We performed all the experimental procedures in accordance with the protocols approved by the University Committee on Use and Care of Animals (UCUCA) at University of Michigan.

Reagents

Cholera toxin (CT; List Biological Laboratories), clinical-grade human serum albumin (HSA; Talecris Biotherapeutics), MDP (Bachem), 8-Br-cAMP (Sigma), N6-benzoyl-cAMP (BioLog Life Science Institute), 8-CPT-2'-O-Me-cAMP (Enzo life sciences), CpG (ODN-1826; Invivogen), MALP-2 (Enzo Life Sciences), and alum (SIGMA) were purchased from the indicated commercial sources.

Immunization protocol and treatment of mice with antibiotics

We anesthetized 6~8-week old age- and sex-matched mice with isoflurane and intranasally immunized the mice with 30 μl of PBS (Gibco) containing 30 μg of HSA and 100 ng of CT using a pipette and tip. For secondary immunization, mice were challenged with HSA (30 μg) and CT (100 ng) four weeks after the primary immunization. Mice were not allocated randomly into experimental groups. The number of animals per group was chosen as the minimum likely required for conclusion of biological significance, established from prior experience. The investigators were not blinded to group allocation during experiments. Mice were euthanized 2 weeks after immunization and plasma, cervical lymph node (CLN), and spleen were obtained for analysis. For experiments involving antibiotic treatment, 5~6 week-old age-and sex-matched mice were intranasally treated with 30 μl of PBS containing ampicillin (1 mg/ml; Sigma), vancomycin (0.5 mg/ml; Pfizer), metronidazole (1 mg/ml; Fagron), and neomycin (1 mg/ml; A.G. Scientific) a week before immunization and given the same antibiotic cocktail in the drinking water ad libitum from one week before immunization to 2 weeks after immunization. For oral immunization, mice were given the same antibiotic cocktail in the drinking water from 4 weeks before immunization to sacrifice and, in the meantime, were intragastrically immunized with 200 μl of PBS containing 10 mg of HSA and 10 μg of CT. For systemic immunization, mice were intraperitoneally injected with 100 μl of PBS containing 100 μg of HSA and various concentrations of CT or 30 μg of HSA and 100 μl of alum. To assess the probiotic effect of isolated bacteria, 5×10^5 c.f.u. of live bacteria were intranasally injected into the nasal cavity together with HSA and CT. In GF experiments, all reagents were autoclaved or passed through 0.2 μm filters (Corning) before immunization. GF mice were given intranasally 30 μg of HSA together with 100 ng of CT, 100 ng of MDP, or 5×10^3 c.f.u. of UV-inactivated bacteria. For establishing *S. sciuri* gnotobiotic mice, 1×10^5 c.f.u./mouse of *S. sciuri* were injected into the nasal cavity of GF

mice 5 days before immunization. No animals or samples were excluded for analyses in the described mouse experiments.

Measurement of HSA-specific antibodies

We measured the levels of HSA-specific total IgG, IgG_1, IgG_{2b}, and IgM in serially diluted serum using a sandwich ELISA method according to the manufacturer's instructions (SBA Clonotyping™ System/AP; SouthernBiotech). The investigators were not blinded to group allocation during experiments.

Restimulation of splenocytes

Splenocytes were isolated from spleen on day 14 after a single immunization as described[49]. Briefly, spleens were mashed through a cell strainer (Falcon) and then the cells were spun down and resuspended in RBC lysis buffer (eBioscience). After 5 m, the cells were rinsed with complete RPMI medium containing 10% heat-inactivated fetal bovine serum, 2-β-mercaptoethanol (50 μM), L-glutamine (2 mM), sodium pyruvate (1 mM), MEM non-essential amino acids, and penicillin-streptomycin (Gibco) and pushed through the cell strainer. Isolated splenocytes (2×10^6 cells/well/48 well plate in 200 μl) were resuspended in complete RPMI medium and restimulated with 500 μg/ml of HSA. After 4 days, culture supernatants were harvested and analyzed for cytokines by ELISA. The investigators were not blinded to group allocation during experiments.

NALT isolation and cell sorting

NALT was isolated from the palate of mice as described[50]. The lymphoid cells were dissociated from NALT by scraping with a surgical knife and forceps, followed by RBC lysis. The cells were then sorted using a FACSAria II (BD Biosciences) instrument and the data analyzed using FlowJo software (TreeStar).

Flow cytometric analysis

Fluorescence-labeled mAb against CD19 (1D3), CD138 (281-2), and IgD (11-26c), CD3 (145-2C11), CD4 (GK1.5), CXCR5 (SPRCL5) PD-1(J43), and CD11c (N418) were from eBioscience. All antibodies were used at 1:200 dilution. Antibody for CD45 (30-F11) was purchased from BD Phamingen. Cell surface fluorescence was measured using a FACSCanto II (BD Biosciences) instrument and the data analyzed using FlowJo software (TreeStar).

ELISPOT assay

ELISPOT assays were performed on the day of CLN isolation to examine antigen-specific IgG producing cells. Immobilon-IP PVDF-based 96-well plates (Millipore) were coated with 100 μg/well of HSA overnight at 4 °C. The plates were blocked with 1% bovine serum albumin for 1 h at room temperature (RT) and then washed 4 times with PBS containing 0.05% Tween 20 (PBST). Lymphocytes from CLNs were incubated with 4×10^5 cells/well for 3 days at 37 °C in a 5% CO_2 incubator. ELISPOT plates were washed 3 times with PBST and 100 μl of biotinylated anti-mouse IgG antibody (Southern biotech) diluted 1:500 in PBST was added to each well. After 2 h incubation at RT, plates were washed 4 times with

PBST and 100 μl of streptavidin-alkaline phosphatase (Southern biotech) diluted 1:1,000 in PBST was added for 2 h. Following washing, ELISPOT plates were developed with Vector blue substrate kit (Vector laboratories Inc.). To stop the reaction, the plates were washed and dried. Spot patterns were analyzed using an ImmunoSpot image analyzer (Cellular Technology). Data are presented as the mean numbers of antigen-specific HSA-specific IgG producing cells per 10^6 lymphocytes from quadruplicate wells.

BMDC *in vitro* stimulation

Bone-marrow-derived dendritic cells (BMDCs) were prepared as previously described[51]. Briefly, bone marrow cells were cultured with media containing 20 ng/ml of GM-CSF (PeproTech) and supplemented with fresh media on day 3 and 5. After 7 days, non-adherent cells were collected as differentiated BMDCs by vigorous aspiration. BMDCs (4×10^5 cells/well/48 well plate in 200 μl) were stimulated with MDP (10 μg/ml), CT (500 ng/ml), and cAMP derivatives (8-Br-cAMP (100 μM), 6-Bnz-cAMP (50 μM), 8-CPT-2'-O-Me-cAMP (50 μM)) for 24 h. Culture supernatants were harvested and cytokines were analyzed by ELISA.

Measurement of Nod2-stimulatory activity

HEK293 cells stably expressing human NOD2 (HEK293-NOD2) and an NF-κB luciferase reporter have been described[29]. The reporter cells (4×10^4 cells/well/96 well plates) were plated in DMEM supplemented with 10% heat-inactivated fetal bovine serum, 2 mM L-glutamine, 1 mM sodium pyruvate, and 1× penicillin-streptomycin (Gibco). The next day, 100 μl of samples including NALF, live bacteria, or UV-inactivated bacteria at a bacterium/HEK293-NOD2 cell ratio of about 1:1 were added to the cells. For live bacteria, gentamicin (50 ng/ml, Gibco) was added to the media 2 h after infection. After 24 h, the reporter cells were lysed with lysis buffer (Promega) and luciferase activity were measured in the lysate according to the manufacturer's instructions (Promega).

Isolation, identification and quantification of bacteria from the nasal cavity

NALF obtained with 100 μl of PBS was collected from adult mice immediately after sacrifice and the NALF was spread on BHI agar plates and cultured at 37 °C under aerobic conditions. Individual bacterial colonies with different morphology were isolated and characterized. The identification of bacterial species was determined by 16S rDNA sequencing of V3–V4 regions as described[52]. Bacterial DNAs were extracted from NALF using E.Z.N.A Stool DNA kit (Omega bio-tek) and then used for real-time PCR with primer sets of universal 16S rDNA.

Real-time PCR

RNA was extracted by using E.Z.N.A. Total RNA kit I (Omega bio-tek) and cDNAs were then made from the isolated RNAs by using the high capacity RNA-to-cDNA kit (Applied Biosystems). The cDNA were used for real-time PCR with primer sets and SYBR Green PCR Master Mix (Applied Biosystems) according to the manufacturer's instruction using the StepOnePlus Real-Time PCR systems (Applied Biosystems). Real-time PCR primers (Invitrogen) were as follows: Nod2 (5'-AACTGTCCAACAATGGCATCAC-3'; 5'-

TTCCCTCGAAGCCAAACCT-3'), GAPDH (5'-TGCGACTTCAACAGCAACTC-3'; 5'-GCCTCTCTTGCTCAGTGTCC-3') and universal 16S rDNA (5'-AGAGTTTGATCCTGGCTCAG-3'; 5'-TGCTGCCTCCCGTAGGAGT-3')[53]. The PCR conditions for mRNA quantification were 95 °C for 10 m, followed by 40 cycles with denaturation at 95 °C for 10 s and annealing and extension at 60 °C for 1 m. An amplification program for bacterial quantification consisted of one cycle at 95 °C for 10 m, 40 cycles at 94 °C for 20 s, 55 °C for 20 s and 72 °C for 50 s, and final one cycle at 94 °C for 15 s. Cycle threshold (Ct) of respective samples were normalized internally using the average Ct value of GAPDH.

Statistical Analyses

No statistical methods were used to predetermine sample size. Statistical analyses were performed using GraphPad Prism software (GraphPad Software). For cytokine comparisons, linear regression with a 95% confidence interval, and unpaired, two-tailed Student's *t*-test were used. When the results from individual animals were analyzed, we examined differences between groups using the non-parametric Mann–Whitney test or Kruskal–Wallis test with a Dunn's *post hoc* test for multiple comparisons. No samples or animals were excluded from the analyses. Differences at $P < 0.05$ were considered to be statistically significant.

Supplementary Material

Refer to Web version on PubMed Central for supplementary material.

Acknowledgments

This work was supported by National Institute of Health Grant (NIH) R01 DK61707 (G. N.), the University of Michigan's Cancer Center Support Grant (5 P30 CA46592) (G. N.) and CRC1182, TP5 and DFG Cluster of Excellence Inflammation at Interfaces (P. R.). We thank M. Zeng for critical review of the manuscript, L. Haynes for animal husbandry and the University of Michigan Germ-Free Animal Core Facility and Host Microbiome Initiative for support.

References

1. Freytag LC, Clements JD. Mucosal adjuvants. Vaccine. 2005; 23:1804–1813. [PubMed: 15734046]
2. Elson CO, Ealding W. Generalized systemic and mucosal immunity in mice after mucosal stimulation with cholera toxin. J. Immunol. 1984; 132:2736–2741. [PubMed: 6233359]
3. Porgador A, Staats HF, Itoh Y, Kelsall BL. Intranasal immunization with cytotoxic T-lymphocyte epitope peptide and mucosal adjuvant cholera toxin: selective augmentation of peptide-presenting dendritic cells in nasal mucosa-associated lymphoid tissue. Infect. Immun. 1998; 66:5876–5881. [PubMed: 9826368]
4. Sunahara RK, Dessauer CW, Whisnant RE, Kleuss C, Gilman AG. Interaction of Gs with the Cytosolic Domains of Mammalian Adenylyl Cyclase. J. Biol. Chem. 1997; 272:22265–22271. [PubMed: 9268375]
5. Lycke N, Tsuji T, Holmgren J. The adjuvant effect of Vibrio cholerae and Escherichia coli heat-labile enterotoxins is linked to their ADP-ribosyltransferase activity. Eur. J. Immunol. 1992; 22:2277–2281. [PubMed: 1381311]
6. Williamson E, Westrich GM, Viney JL. Modulating dendritic cells to optimize mucosal immunization protocols. J. Immunol. 1999; 163:3668–3675. [PubMed: 10490961]

7. Datta SK, et al. Mucosal adjuvant activity of cholera toxin requires Th17 cells and protects against inhalation anthrax. Proc. Natl. Acad. Sci. U S A. 2010; 107:10638–10643. [PubMed: 20479237]
8. Braun MC, He J, Wu CY, Kelsall BL. Cholera Toxin Suppresses Interleukin (IL)-12 Production and IL-12 Receptor 1 and 2 Chain Expression. J. Exp. Med. 1999; 189:541–552. [PubMed: 9927516]
9. Xu-Amano J. Helper T cell subsets for immunoglobulin A responses: oral immunization with tetanus toxoid and cholera toxin as adjuvant selectively induces Th2 cells in mucosa associated tissues. J. Exp. Med. 1993; 178:1309–1320. [PubMed: 8376936]
10. Yamamoto S, et al. A nontoxic mutant of cholera toxin elicits Th2-type responses for enhanced mucosal immunity. Proc. Natl. Acad. Sci. U S A. 1997; 94:5267–5272. [PubMed: 9144226]
11. la Sala A, et al. Cholera toxin inhibits IL-12 production and CD8alpha+ dendritic cell differentiation by cAMP-mediated inhibition of IRF8 function. J. Exp. Med. 2009; 206:1227–1235. [PubMed: 19487420]
12. Li X, et al. Divergent requirement for Galphas and cAMP in the differentiation and inflammatory profile of distinct mouse Th subsets. J. Clin. Invest. 2012; 122:963–973. [PubMed: 22326954]
13. Mattsson J, et al. Cholera toxin adjuvant promotes a balanced Th1/Th2/Th17 response independently of IL-12 and IL-17 by acting on Gsalpha in CD11b DCs. Mucosal Immunol. 2014
14. Shaw MH, Reimer T, Kim YG, Nunez G. NOD-like receptors (NLRs): bona fide intracellular microbial sensors. Curr. Opin. Immunol. 2008; 20:377–382. [PubMed: 18585455]
15. Inohara N, et al. Host recognition of bacterial muramyl dipeptide mediated through NOD2. Implications for Crohn's disease. J. Biol. Chem. 2003; 278:5509–5512. [PubMed: 12514169]
16. Girardin SE, et al. Nod2 is a general sensor of peptidoglycan through muramyl dipeptide (MDP) detection. J. Biol. Chem. 2003; 278:8869–8872. [PubMed: 12527755]
17. Park JH, et al. RICK/RIP2 Mediates Innate Immune Responses Induced through Nod1 and Nod2 but Not TLRs. J. Immunol. 2007; 178:2380–2386. [PubMed: 17277144]
18. Hasegawa M, et al. A critical role of RICK/RIP2 polyubiquitination in Nod-induced NF-κB activation. EMBO J. 2008; 27:373–383. [PubMed: 18079694]
19. Pavot V, et al. Cutting edge: New chimeric NOD2/TLR2 adjuvant drastically increases vaccine immunogenicity. J. Immunol. 2014; 193:5781–5785. [PubMed: 25392526]
20. Magalhaes JG, et al. Nod2-dependent Th2 polarization of antigen-specific immunity. J. Immunol. 2008; 181:7925–7935. [PubMed: 19017983]
21. Fritz JH, et al. Nod1-mediated innate immune recognition of peptidoglycan contributes to the onset of adaptive immunity. Immunity. 2007; 26:445–459. [PubMed: 17433730]
22. Allen EK, et al. Characterization of the nasopharyngeal microbiota in health and during rhinovirus challenge. Microbiome. 2014; 2:22. [PubMed: 25028608]
23. Warner N, Nunez G. MyD88: a critical adaptor protein in innate immunity signal transduction. J. Immunol. 2013; 190:3–4. [PubMed: 23264668]
24. Kawai T, Akira S. Toll-like Receptors and Their Crosstalk with Other Innate Receptors in Infection and Immunity. Immunity. 2011; 34:637–650. [PubMed: 21616434]
25. Reinhardt RL, Liang HE, Locksley RM. Cytokine-secreting follicular T cells shape the antibody repertoire. Nat. Immunol. 2009; 10:385–393. [PubMed: 19252490]
26. Eto D, et al. IL-21 and IL-6 are critical for different aspects of B cell immunity and redundantly induce optimal follicular helper CD4 T cell (Tfh) differentiation. PLoS One. 2011; 6:e17739. [PubMed: 21423809]
27. Karnowski A, et al. B and T cells collaborate in antiviral responses via IL-6, IL-21, and transcriptional activator and coactivator, Oct2 and OBF-1. J. Exp. Med. 2012; 209:2049–2064. [PubMed: 23045607]
28. de Rooij J, et al. Epac is a Rap1 guanine-nucleotide-exchange factor directly activated by cyclic AMP. Nature. 1998; 396:474–477. [PubMed: 9853756]
29. Warner N, et al. A Genome-Wide siRNA Screen Reveals Positive and Negative Regulators of the NOD2 and NF-κB Signaling Pathways. Cell Signal. 2013; 6 rs3-rs3.
30. Ivanov II, et al. Specific microbiota direct the differentiation of IL-17-producing T-helper cells in the mucosa of the small intestine. Cell Host Microbe. 2008; 4:337–349. [PubMed: 18854238]

31. Shulzhenko N, et al. Crosstalk between B lymphocytes, microbiota and the intestinal epithelium governs immunity versus metabolism in the gut. Nat. Med. 2011; 17:1585–1593. [PubMed: 22101768]
32. Abt MC, et al. Commensal bacteria calibrate the activation threshold of innate antiviral immunity. Immunity. 2012; 37:158–170. [PubMed: 22705104]
33. Mazmanian SK, Round JL, Kasper DL. A microbial symbiosis factor prevents intestinal inflammatory disease. Nature. 2008; 453:620–625. [PubMed: 18509436]
34. Ellouz F, Adam A, Ciorbaru R, Lederer E. Minimal structural requirements for adjuvant activity of bacterial peptidoglycan derivatives. Biochem. Biophys. Res. Commun. 1974; 59:1317–1325. [PubMed: 4606813]
35. Magalhaes JG, et al. Nucleotide oligomerization domain-containing proteins instruct T cell helper type 2 immunity through stromal activation. Proc. Natl. Acad. Sci. U S A. 2011; 108:14896–14901. [PubMed: 21856952]
36. Duan W, et al. Innate signals from Nod2 block respiratory tolerance and program T(H)2-driven allergic inflammation. J. Allergy Clin. Immunol. 2010; 126:1284–1293. e1210. [PubMed: 21051079]
37. Ma CS, et al. Early commitment of naive human CD4+ T cells to the T follicular helper (TFH) cell lineage is induced by IL-12. Immunol. Cell Biol. 2009; 87:590–600. [PubMed: 19721453]
38. Schmitt N, et al. Human dendritic cells induce the differentiation of interleukin-21-producing T follicular helper-like cells through interleukin-12. Immunity. 2009; 31:158–169. [PubMed: 19592276]
39. Jiang V, Jiang B, Tate J, Parashar UD, Patel MM. Performance of rotavirus vaccines in developed and developing countries. Hum. Vaccine. 2010; 6:532–542.
40. Levine MM. Immunogenicity and efficacy of oral vaccines in developing countries: lessons from a live cholera vaccine. BMC Biol. 2010; 8:129. [PubMed: 20920375]
41. Lopman BA, et al. Understanding reduced rotavirus vaccine efficacy in low socio-economic settings. PLoS One. 2012; 7:e41720. [PubMed: 22879893]
42. Grassly NC, et al. Mucosal immunity after vaccination with monovalent and trivalent oral poliovirus vaccine in India. J. Infect. Dis. 2009; 200:794–801. [PubMed: 19624278]
43. Johnson RA, et al. Comparison of immune responses to the O-specific polysaccharide and lipopolysaccharide of Vibrio cholerae O1 in Bangladeshi adult patients with cholera. Clin. Vaccine Immunol. 2012; 19:1712–1721. [PubMed: 22993410]
44. Leung DT, et al. Comparison of memory B cell, antibody-secreting cell, and plasma antibody responses in young children, older children, and adults with infection caused by Vibrio cholerae O1 El Tor Ogawa in Bangladesh. Clin. Vaccine Immunol. 2011; 18:1317–1325. [PubMed: 21697337]
45. Yatsunenko T, et al. Human gut microbiome viewed across age and geography. Nature. 2012; 486:222–227. [PubMed: 22699611]
46. Korpe PS, Petri WA Jr. Environmental enteropathy: critical implications of a poorly understood condition. Trends Mol. Med. 2012; 18:328–336. [PubMed: 22633998]
47. Chattha KS, Vlasova AN, Kandasamy S, Rajashekara G, Saif LJ. Divergent immunomodulating effects of probiotics on T cell responses to oral attenuated human rotavirus vaccine and virulent human rotavirus infection in a neonatal gnotobiotic piglet disease model. J. Immunol. 2013; 191:2446–2456. [PubMed: 23918983]
48. Oh JZ, et al. TLR5-mediated sensing of gut microbiota is necessary for antibody responses to seasonal influenza vaccination. Immunity. 2014; 41:478–492. [PubMed: 25220212]

Methods References

49. Kim D, et al. Suppression of Allergic Diarrhea in Murine Ovalbumin-Induced Allergic Diarrhea Model by PG102, a Water-Soluble Extract Prepared from *Actinidia arguta*. Int. Arch. Allergy Immunol. 2009; 150:164–171. [PubMed: 19439982]
50. Wu HY, Nguyen HH, Russell MW. Nasal lymphoid tissue (NALT) as a mucosal immune inductive site. Scandinavian journal of immunology. 1997; 46:506–513. [PubMed: 9393634]

51. Franchi L, Eigenbrod T, Nunez G. Cutting edge: TNF-alpha mediates sensitization to ATP and silica via the NLRP3 inflammasome in the absence of microbial stimulation. J. Immunol. 2009; 183:792–796. [PubMed: 19542372]

52. Hasegawa M, et al. Transitions in oral and intestinal microflora composition and innate immune receptor-dependent stimulation during mouse development. Infect. Immun. 2010; 78:639–650. [PubMed: 19933833]

53. Ubeda C, et al. Vancomycin-resistant Enterococcus domination of intestinal microbiota is enabled by antibiotic treatment in mice and precedes bloodstream invasion in humans. The Journal of clinical investigation. 2010; 120:4332–4341. [PubMed: 21099116]

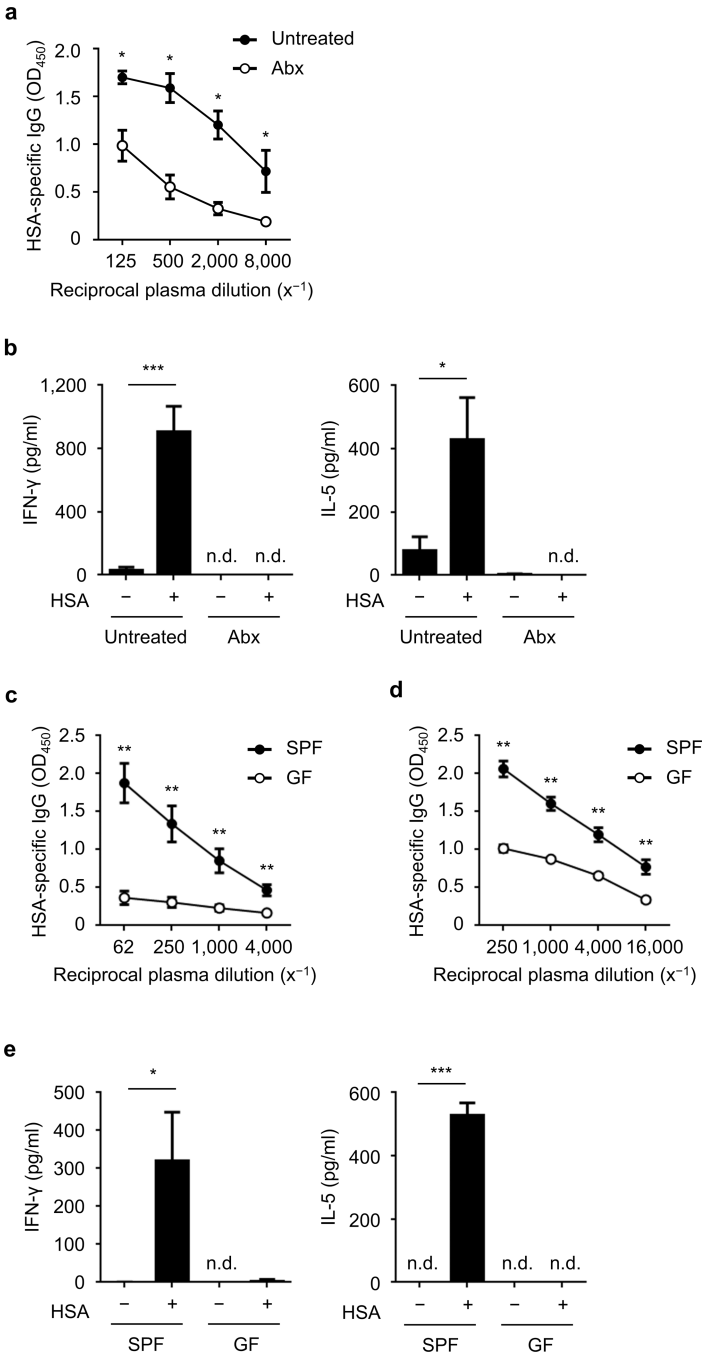

Figure 1. Symbiotic bacteria promote the adjuvant activity of cholera toxin after nasal immunization

(**a**) Relative amount of HSA-specific IgG (OD_{450}) in serially diluted plasma from antibiotic (Abx)-treated mice and untreated group (each group $n = 4$) on day 14 after intranasal immunization with HSA and CT. (**b**) Concentration of IFN-γ and IL-5 in the supernatant of splenocytes (measured in triplicate) from antibiotic-treated mice and untreated group on day 14 post-immunization, after restimulation with or without HSA for 4 d. (**c, d**) HSA-specific IgG in the plasma of GF and SPF mice (each group $n = 5$) on day 14 after primary and

secondary immunization. (**e**) Concentration of IFN-γ and IL-5 (measured in triplicate) in the supernatant of splenocytes isolated from immunized GF and SPF mice on day 14 post-primary immunization, after restimulation with and without antigen for 4 d. The results are representative of at least two independent experiments. Values represent mean ± s.e.m. (**a, c, d**) or ± s.d. (**b, e**). *$P < 0.05$, **$P < 0.01$, and ***$P < 0.001$ by Mann-Whitney test (**a, c, d**) and by Student's *t*-test (**b, e**). n.d., not detected.

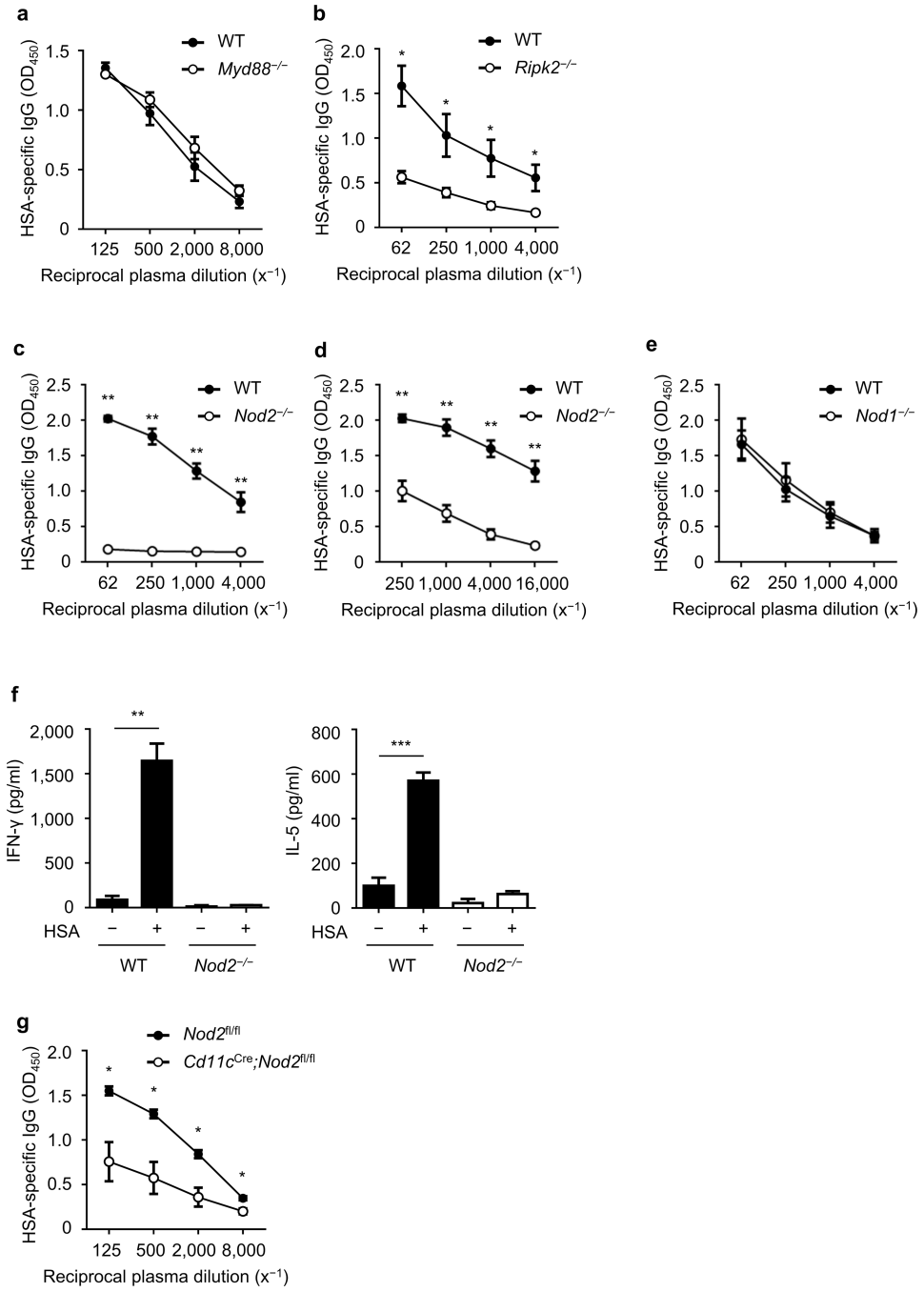

Figure 2. The adjuvant activity of cholera toxin is mediated by CD11c^{+} cells via Nod2

(**a–c**) Relative amounts of HSA-specific IgG (OD_{450}) in serially diluted plasma from *Myd88*$^{-/-}$ ($n = 5$) (**a**), *Ripk2*$^{-/-}$ ($n = 4$) (**b**), *Nod2*$^{-/-}$ ($n = 5$) (**c–d**), *Nod1*$^{-/-}$ ($n = 5$) (**e**) and *Cd11c*^{Cre};*Nod2*$^{fl/fl}$ mice ($n = 4$) (**g**), and WT ($n = 4$ or 5) or *Nod2*$^{fl/fl}$ littermates ($n = 4$) on day 14 after intranasal immunization with HSA and CT (**a–c, e, g**) or after secondary challenge with HSA and CT (**d**). (**f**) Concentration of IFN-γ and IL-5 in the supernatants of splenocytes (measured in triplicate) from *Nod2*$^{-/-}$ mice and WT animals on day 14 post-primary immunization, after restimulation with and without antigen for 4 d. The results are

representative of at least two independent experiments. Data are shown as means ± s.e.m. (**a–e, g**) or ± s.d. (**f**). $*P < 0.05$, $**P < 0.01$, and $***P < 0.001$ by Mann-Whitney test (**a–e, g**) and by Student's *t*-test (**f**).

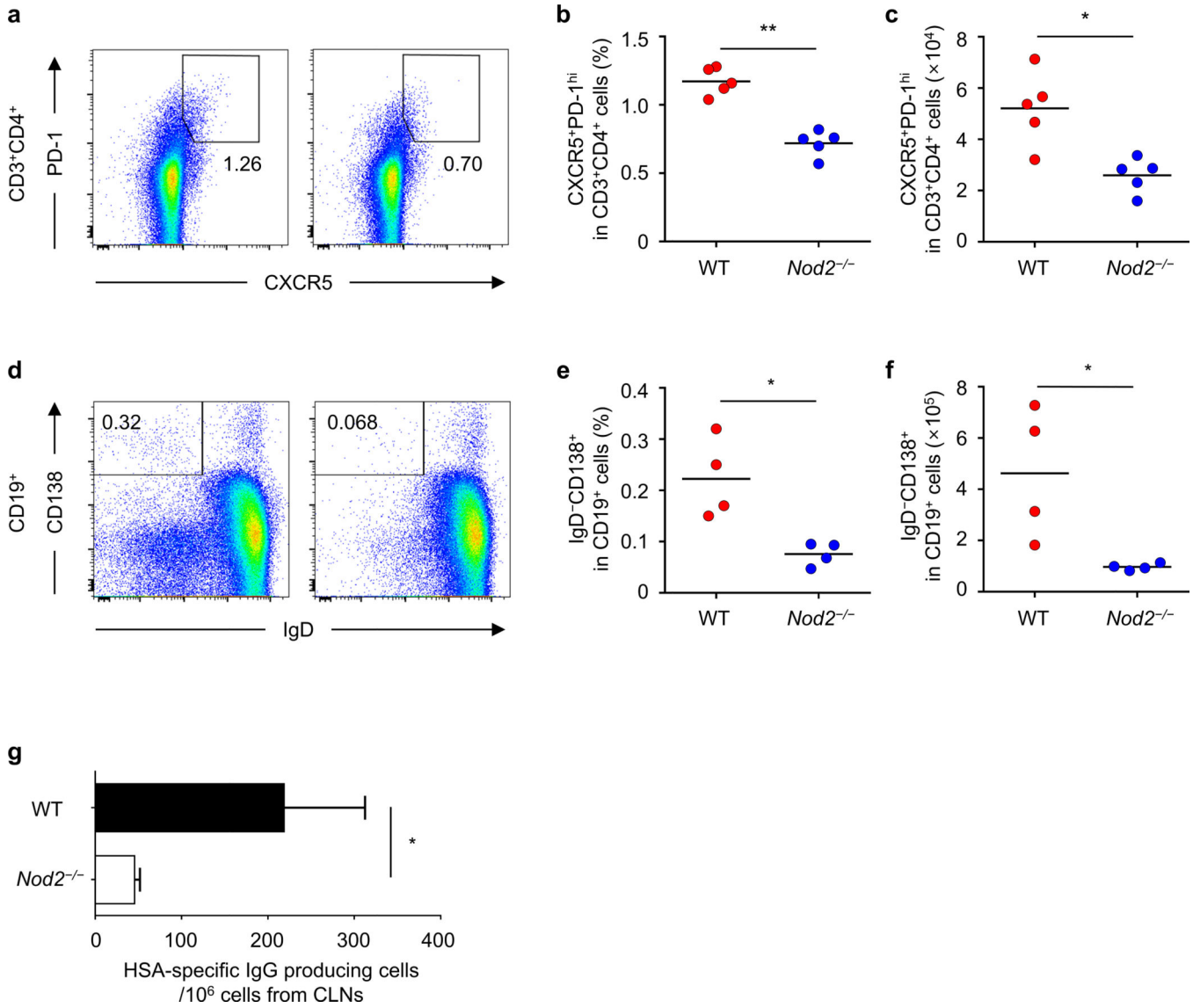

Figure 3. Nod2 is required for the generation of T_{FH} and plasma cells after nasal immunization with antigen and cholera toxin

The percentage and total number of T_{FH} cells ($CXCR5^+PD\text{-}1^{hi}$) (**a–c**) and plasma cells ($CD138^+IgD^-$) (**d–f**) from the cervical lymph nodes (CLNs) on day 14 post-immunization. (**a, d**) The plots shown for T_{FH} cells were gated on $CD3^+CD4^+$ T cells and the plots for plasma cells were gated on $CD19^+$ cells (left panels, WT and right panels, *Nod2*$^{-/-}$). (**b, c, e, f**) Each dot represents an individual mouse and the means are displayed by a line. (**g**) Number of cells producing HSA-specific IgG among total cells obtained from CLNs of WT or *Nod2*$^{-/-}$ mice on day 14 post-immunization. Results are representative of at least two independent experiments. $*P < 0.05$ and $**P < 0.01$ by Mann-Whitney test (**b, c, e, f**) and by Student's *t*-test (**g**).

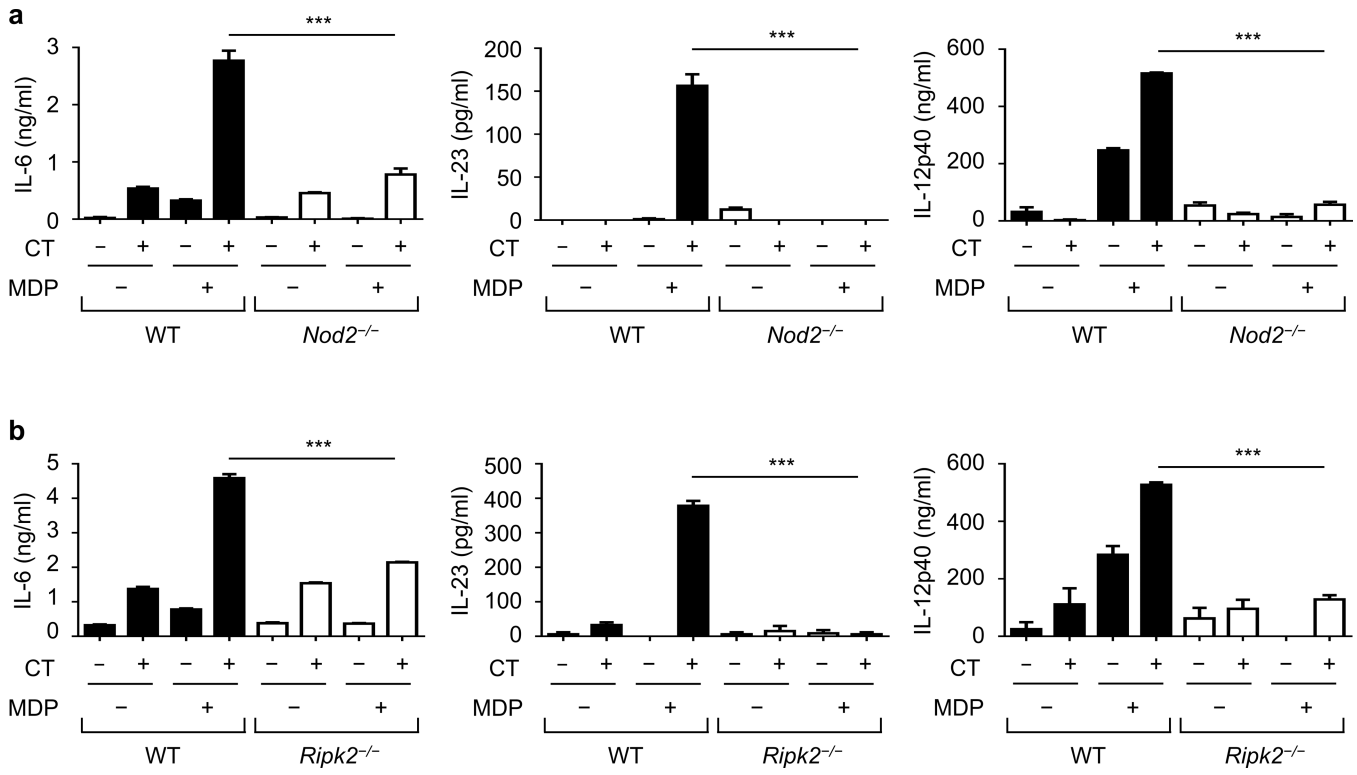

Figure 4. Cholera toxin enhances MDP-induced cytokine production in DCs

Concentration of cytokines in the supernatant of bone-marrow-derived dendritic cells (BMDCs) (measured in triplicate) from WT and *Nod2*$^{-/-}$ (**a**) or *Ripk2*$^{-/-}$ (**b**) mice, after treatment with indicated stimuli for 24 h. Results are representative of at least three independent experiments. Data are expressed as the mean ± s.d. ***$P < 0.001$ by Student's *t*-test.

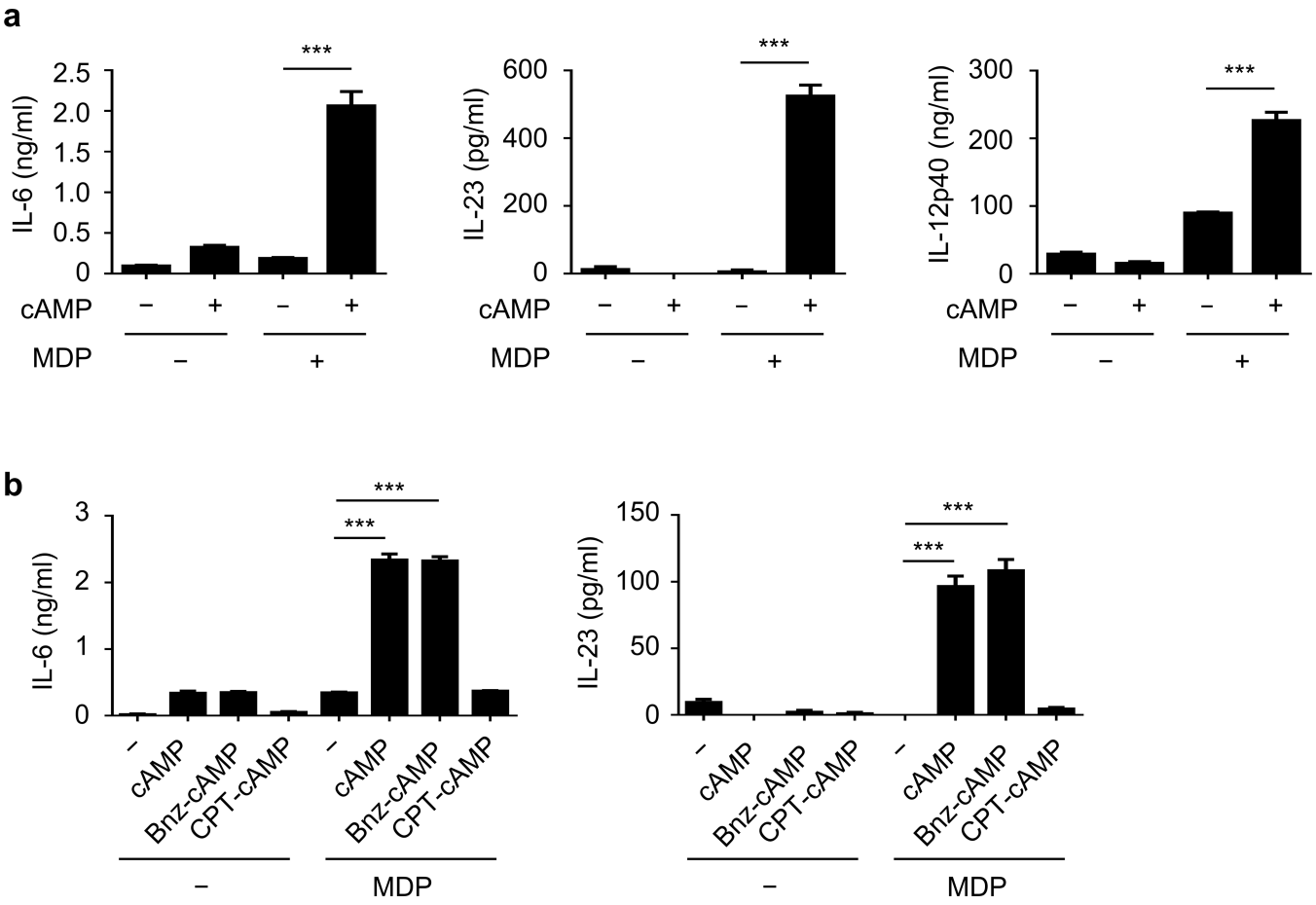

Figure 5. Cholera toxin promotes Nod2 activation via cAMP/PKA signaling

(**a**) Concentration of cytokines in the supernatant of BMDC (measured in triplicate) treated with the indicated stimuli for 24 h. (**b**) Concentration of cytokines in the supernatant of BMDM (measured in triplicate) treated with 8-Br-cAMP (cAMP), N6-benzoyl-cAMP (Bnz-cAMP), or 8-CPT-2'-O-Me-cAMP (CPT-cAMP) in the presence or absence of MDP for 24 h. The results are representative of at least three independent sets of experiments. Data are expressed as the mean ± s.d. ***$P < 0.001$ by Student's t-test.

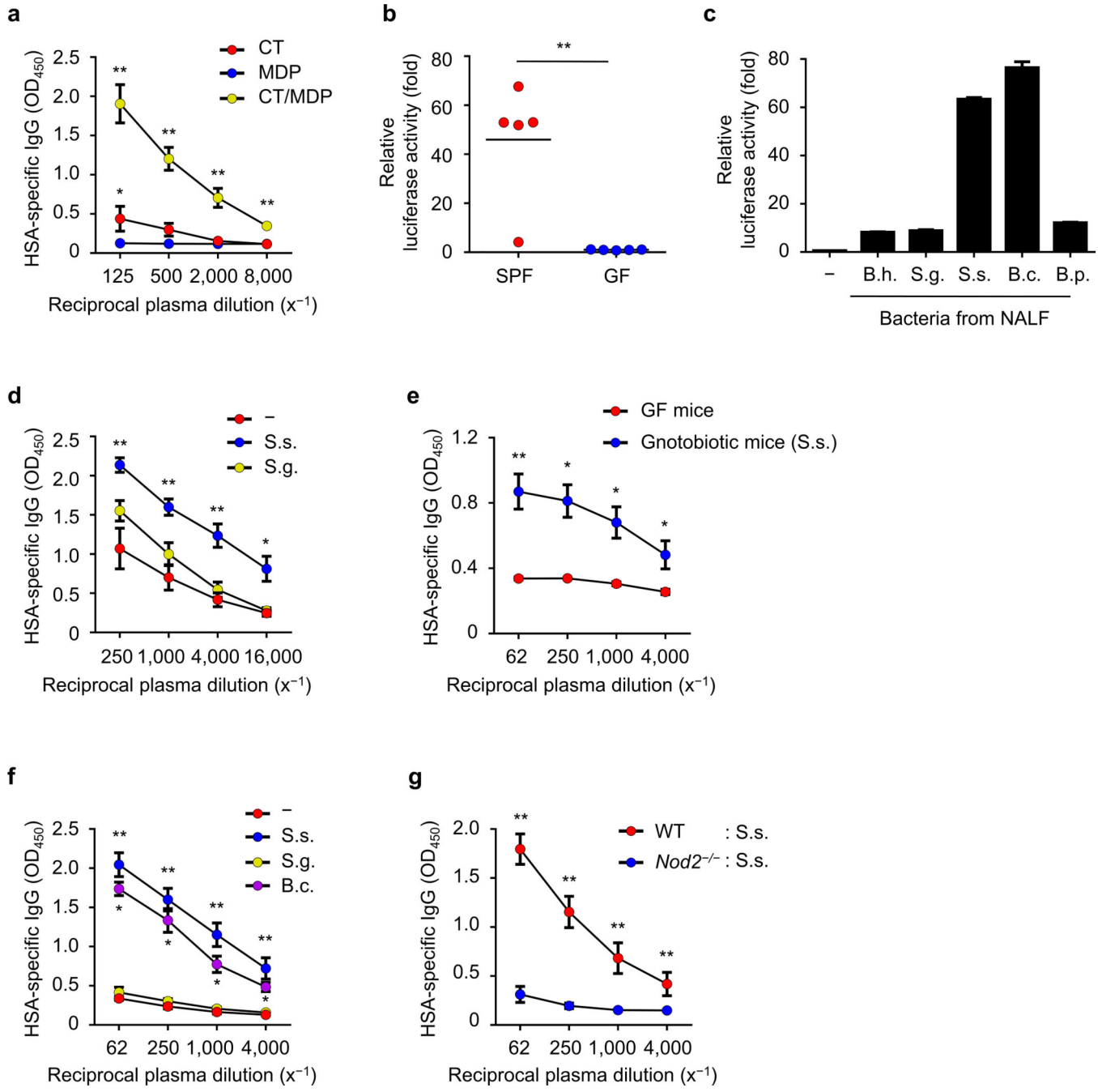

Figure 6. Nod2-stimulatory bacteria promote the adjuvant activity of cholera toxin

(**a**) Relative levels of HSA-specific IgG in plasma of GF mice (each group $n = 5$) intranasally immunized with indicated stimuli in the presence HSA on day 14 post-immunization. (**b**) Nod2-stimulatory activity in NALF from SPF or GF mice. Each dot represents an individual mouse and the mean value is displayed by a line (**c**) Nod2-stimulatory activity in indicated bacteria isolated from NALF. B. h., *Bordetella hinzii*; S. g., *Staphylococcus gallinarum*; S. s., *Staphylococcus sciuri*; B. c., *Bacillus clausii*; B. p., *Bacillus pumilus*. (**d–f**) Relative amounts of HSA-specific IgG were analyzed in plasma on

day 14 post-immunization. (**d**) SPF mice (each group $n = 5$) were intranasally immunized with HSA and CT together with live *S. sciuri* or *S. gallinarum*. (**e**) GF ($n = 5$) and gnotobiotic mice ($n = 6$) monocolonized with *S. sciuri* were intranasally given HSA and CT on day 5 after monocolonization. (**f**) GF mice were intranasally treated with HSA and CT together with UV-inactivated *S. sciuri, S. gallinarum*, or *B. clausii*. (**g**) The relative levels of HSA-specific IgG were examined in plasma on day 14 post-immunization of WT GF ($n = 5$) and *Nod2*$^{-/-}$ GF ($n = 6$) mice given UV-inactivated *S. sciuri*, HSA, and CT. Data represent means ± s.e.m. (**a, d–g**) or ± s.d. (**c**). $*P < 0.05$ and $**P < 0.01$ by Kruskal-Wallis test with *post-hoc* Dunn's test (**a, d, f**), by Mann-Whitney test (**b, g**) and by Student's *t*-test (**c**). $*P < 0.05$ between CT and MDP groups by Mann-Whitney test (a).